JOURNAL OF MATERIALS SCIENCE 27 (1992) 587–591

Characterization of internal structure in Y–TZP powder compacts

J.-Y. KIM, M. MIYASHITA, M. INOUE, N. UCHIDA, K. SAITO, K. UEMATSU
Department of Chemistry, Faculty of Engineering, Nagaoka University of Technology, Kamitomioka, Nagaoka, Niigata, Japan 940-21

The internal structure of yttrium-doped tetragonal zirconia powder compact was characterized using the immersion liquid technique, mercury porosimetry, scanning electron microscopy, and a compaction test. The specimens examined were prepared by pressing spray-dried granules at various pressures from 5–600 MPa. The immersion liquid technique had numerous potential advantages, over the other methods for evaluating defects of 1–10 μm in size. With this technique, intergranular interfaces and pores were found to be present even in the specimen prepared at 600 MPa. A feature, which is considered to be an agglomerate, was also found. The significance of the large defects on ceramic processing, as well as a comparison of the technique with the other methods, is presented.

1. Introduction

Processing defects may originate during forming processes and persist to critical defects in sintered ceramics [1]. These forming-related defects may critically limit the performance and reliability of the final products. Analytical characterization of these defects is a prerequisite for the development of high-performance ceramics, because it is very crucial in eliminating or controlling these defects to determine the relationship between flaw size and population and processing variables. Various characterization techniques have been proposed [2–5]. However, no single technique provides full characterization of defects in green compacts.

Recently, Uematsu *et al.* [6–8] developed "an immersion liquid technique" for characterizing spray-dried granules and green compacts of alumina, by which spray-dried granules or green compacts, made transparent by immersion in a liquid, are examined using a traditional optical microscope under transmitted light. The achievement of a "transparent granule or green compact" is based on the reduced internal reflection in the presence of the immersion liquid which has a refractive index close to that of alumina ($n = 1.76$). The procedure is simple, quick and does not require any special equipment. After examining spray-dried granules and powder compacts of alumina using this technique, Uematsu *et al.* found that the direct internal image provides much more detailed information than other existing techniques for 1–10 μm sized defects. More recently, we examined applicability of this unique technique for observing the internal structure of spray-dried yttria-doped tetragonal zirconia (Y–TZP) polycrystal granules which have a relatively large refractive index ($n = 2.15$–2.22) [9]. By using an immersion liquid ($n = 2.02$) with a refractive index closer to that of the powder, clear observation of the internal structure was possible.

This paper presents information obtained on characteristics of the green compacts for the development of Y–TZP with a higher strength. The immersion liquid technique applied to this study again provides much more detailed information on 1–10 μm sized defects. The present work aims (1) to characterize the internal structure of Y–TZP powder compacts more completely by incorporating information obtained by the technique with that from other conventional techniques, and (2) to examine the effect of the forming pressure on the internal structure of Y–TZP powder compacts.

2. Experimental procedure

A commercial spray-dried 3 mol % yttria-doped zirconia granule was used as a starting material. According to the supplier, it has two phases (80% tetragonal + 20% monoclinic), average particle size 0.3 μm (average crystallite size 240 nm) and average granule size 60 μm. The as-received powder granule was uniaxially pressed into a pellet (14 mm diameter × 6 mm) at 5 MPa and then isostatically pressed at various pressures from 5–600 MPa. To burn out the binder, the compact was heated to 800 °C at 1 °C min^{-1} and kept at this temperature for 2 h. For immersion liquids, yellow phosphorus–sulphur–methylene iodide (8:1:1 by weight fraction) was prepared. The refractive index of the liquid, determined by the minimum deviation method, was 2.02. Thinned specimens (0.2 mm) were immersed in the liquid and evacuated for 10 min. The transparent powder compacts prepared were examined under an optical microscope with transmitted light. To examine internal structure along the vertical direction, the specimen-to-lens distance was varied at 10 μm intervals from the top to the bottom surface of the thinned specimen. The internal structure of the powder compact was also examined on the fracture

0022–2461/92 $03.00 + .12

surface by SEM, for comparison. The pore size distribution was determined by mercury porosimetry. The green densities of the specimens were determined from their dimensions and weights, and were compared with those calculated by mercury intrusion.

3. Results

Fig. 1 shows a series of observations along the vertical direction for an immersed thinned specimen which was formed at 5 MPa. By varying the specimen-to-lens distance, a three-dimensional representation could be generated from a series of two-dimensional images. These micrographs show a characteristic feature of round shapes, which are distributed three-dimensionally in powder compacts. The round shapes suggest that the feature corresponds to unfractured granules which survived compaction. The sharp boundary line suggests a very thin boundary between the unfractured granule and the surrounding matrix. The boundary is visible only when viewed from the tangential direction; the curved line represents the maximum diameter of the granules. At this pressure, many granules retained their original shape after compaction.

Fig. 2 shows similar observations for specimens formed at various pressures. With increasing pressure, the granules are deformed and packed more tightly. The void spaces between the granules become narrowed and their concentration decreases with increasing pressure. The detection of voids becomes increasingly difficult with increasing pressure. At 20 MPa, the round shapes corresponding to unfractured granules is often found. Above 100 MPa, the detection of the round shapes is difficult. However, intergranular interfaces and pores are still found at granule boundaries, even at an applied pressure of 600 MPa, as shown in the micrograph.

Fig. 3 shows a more detailed micrograph of the internal structure of an immersed thinned specimen which was formed at 600 MPa. An intergranular interface (A) and a pore (B) were found at granule boundaries. The other morphological feature (C), which is considered to be an agglomerate, was also found.

Fig. 4 shows scanning electron micrographs of fracture surfaces of specimens which were formed at various pressures. At a low forming pressure, many round features were found on the fracture surface, showing that many granules were not fractured and preserved in the powder compact. With increasing pressure, less rounded features were evident on the fracture surface and its roughness tended to decrease.

Fig. 5 shows cumulative pore size distribution in powder compacts prepared at various pressures. Clearly, the majority of pores have a size below 1 μm. With increasing forming pressure, the total volume of pores decreases and the pore size, corresponding to a sharp rise of cumulative pore size, also decreases. For example, the curve rises sharply at 100 and 30 nm in powder compacts prepared at 5 and 600 MPa, respectively. There is also a small, but finite, number of pores in the region exceeding 1 μm for all specimens.

Fig. 6 shows differential pore size distribution for powder compacts prepared at various forming pressures. The most frequent pore size decreases with increasing pressure; 61 nm at 5 MPa, 59 nm at 20 MPa, 50 nm at 40 MPa, 44 nm at 100 MPa, 39 nm at 300 MPa and 33 nm at 600 MPa. Pore size distribution also becomes narrowed with increased pressure. Large pores with size exceeding 1 μm are clearly present in all specimens, but their accurate characterization was difficult. No correlation was found between the pore volume and pressure because of uncertainty in the measurements.

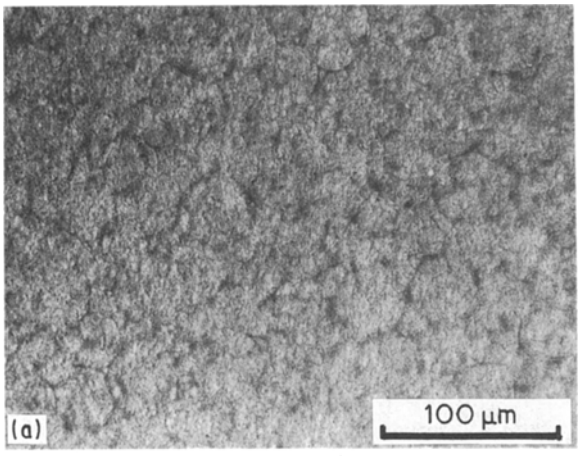

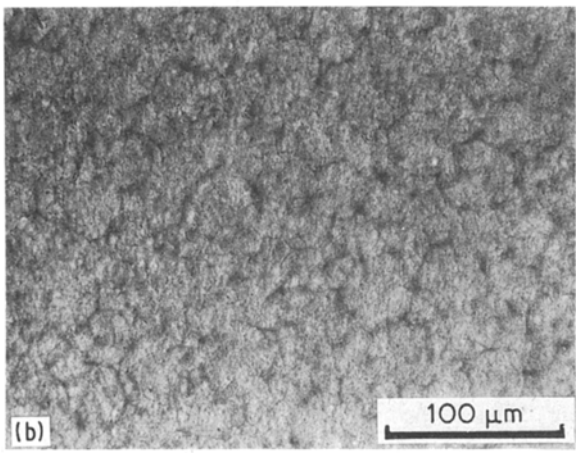

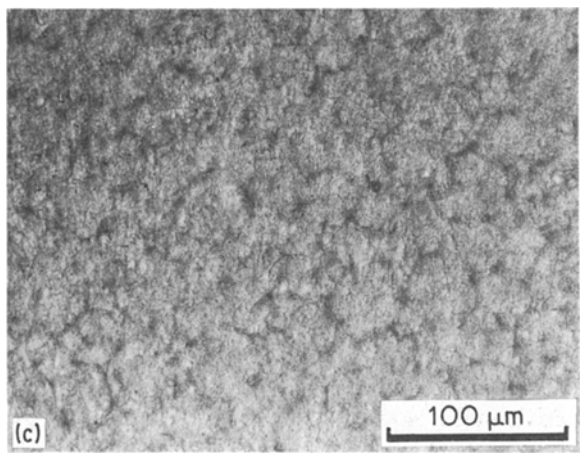

Figure 1 A series of transmission optical micrographs showing the internal structure of a powder compact prepared at a forming pressure of 5 MPa.

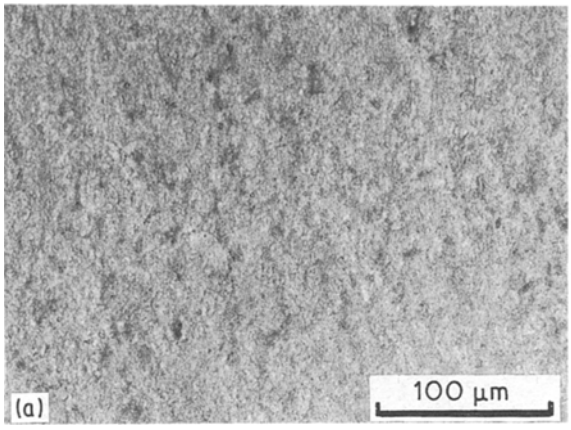

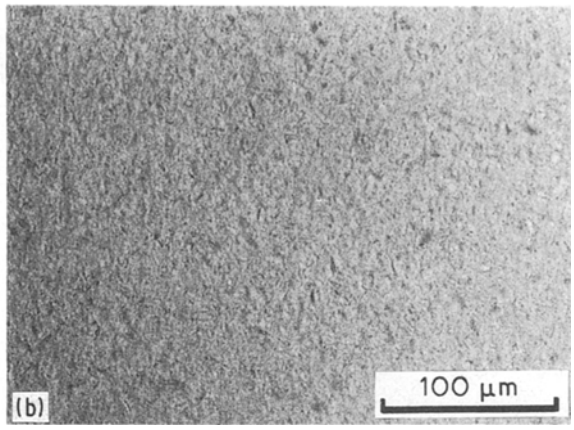

Figure 2 Effect of forming pressure on the internal structure of powder compacts observed directly by transmission optical microscope: (a) 20 MPa; (b) 100 MPa; (c) 600 MPa.

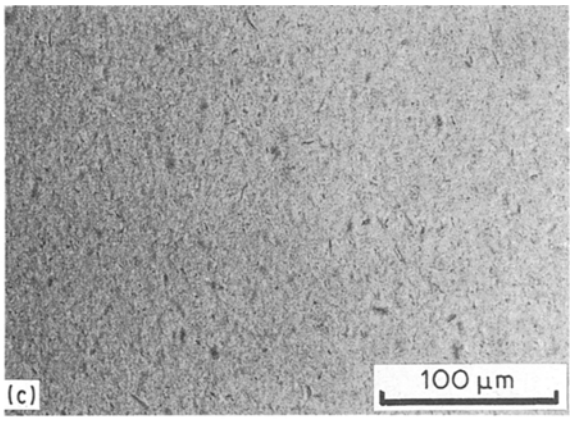

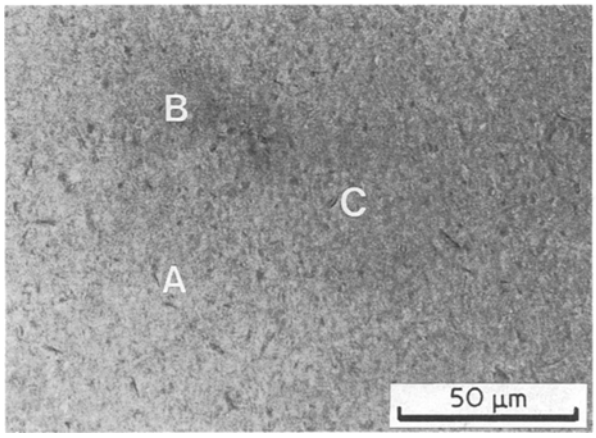

Figure 3 Detailed internal structure of a powder compact prepared at a forming pressure of 600 MPa.

Fig. 7 shows the effect of forming pressure on green densities of specimens, which were determined from their dimensions and weights. The green densities determined agreed well with those calculated by mercury intrusion. The densities increased with increasing forming pressure. It was found that a linear relation existed between a logarithm of pressure and green density.

4. Discussion

Large processing defects of the powder compacts examined include agglomerates and large voids, such as intergranular interfaces and pores. Agglomerates can cause the development and enlargement of large voids during subsequent processing steps. When the green density of the matrix is less than that of agglomerate, the matrix will densify more rapidly and thereby a tensile stress will be generated in the matrix around the agglomerate, resulting in radial crack-like voids during the sintering process. When the green density of the agglomerate is less than that of the matrix, the agglomerate will densify more rapidly, resulting in circumferential crack-like voids between agglomerate and the matrix during the sintering process [10]. Although it is uncertain whether or not the agglomerates found in this study have a higher green density than the matrix, they can form crack-like voids because of their different shrinkage rates relative to the surrounding matrix. The crack-like voids might be potential fracture origins.

Large voids such as intergranular interfaces and pores are known to be very unfavourable in the processing of high-performance ceramics. Once large voids are formed in the green compacts, their elimination by sintering is difficult. They are thermodynamically stable, and do not shrink during the densification process [11–13]. If they persist through the subsequent processing steps, they may act as critical flaws detrimental to properties of the final products.

The present method is superior to SEM in detecting processing defects, at least for their size levels and population examined in this study. SEM gives information only at the surface, whereas the present method provides information throughout the entire volume of the specimen. The chance of detecting processing defects is very low with SEM, particularly in high-performance ceramics with low defect populations.

The pore size distribution determined by mercury porosimetry suggests that the small matrix pores represent the majority of total pore volume fractions. The total volume of pores and the most frequent pore size decrease with increasing forming pressure. This behaviour clearly reflects the reduced interparticle distance with increasing pressure. There may be uncertainty in mercury porosimetry measurements of large pores due

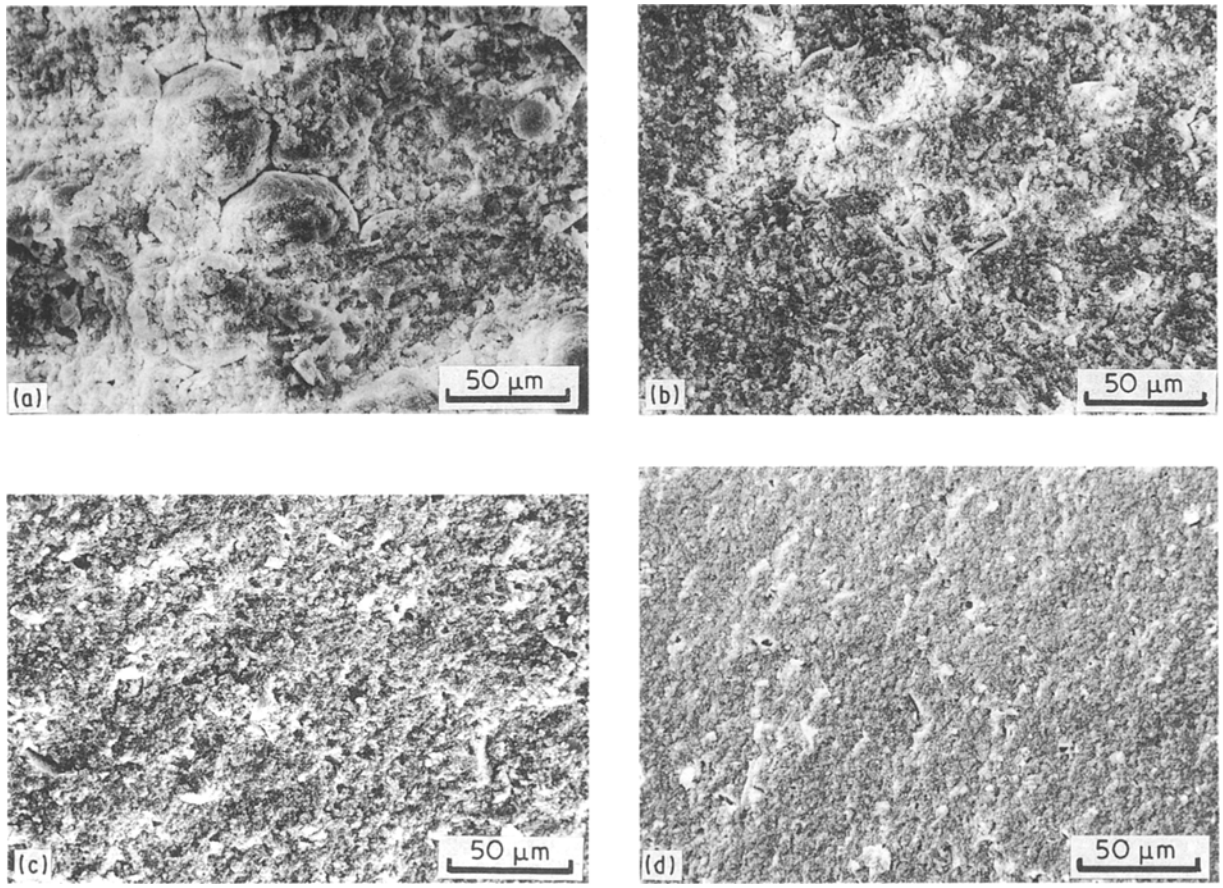

Figure 4 Scanning electron micrographs of fracture surface of powder compacts prepared at various forming pressures: (a) 5 MPa; (b) 20 MPa; (c) 100 MPa; (d) 600 MPa.

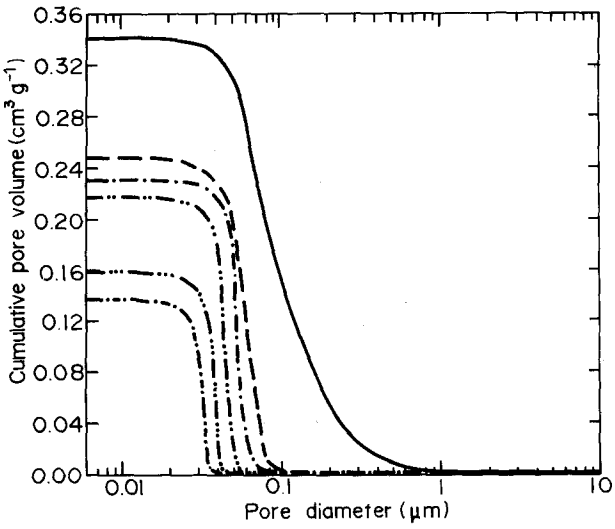

Figure 5 Cumulative pore size distribution of powder compacts prepared at various forming pressures (MPa): (——) 5; (— —) 20; (— · —) 40; (— ·· —) 100; (— ··· —) 300; (— · – · —) 600.

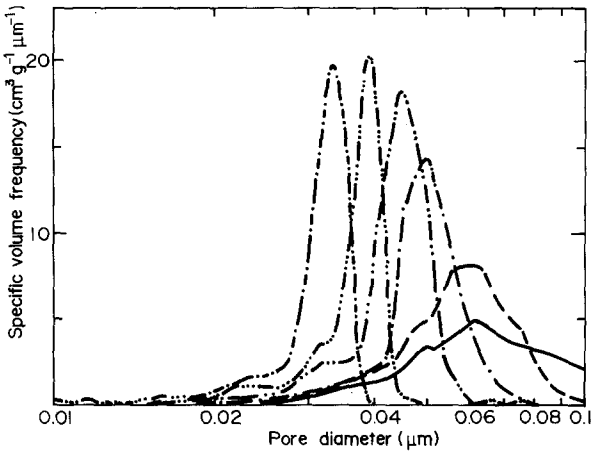

Figure 6 Differential pore size distribution of powder compacts prepared at various forming pressures (MPa): (——) 5; (— —) 20; (— · —) 40; (— ·· —) 100; (— ··· —) 300; (— · – · —) 600.

to mercury intrusion from the surface of the specimen [14]. The method cannot provide clear insight into the large defects found by the immersion liquid technique. Nevertheless, it may still be a standard method for examining ceramic green compacts. The method is particularly powerful for characterizing small pores with a size below 1 μm.

The compaction test of granules was often used in studying the forming process. In general, the compaction mechanism for spray-dried powders can be divided into three processes [15]: (1) rearrangement of granules to improve packing density; (2) reduction of the void volume between granules by plastic deformation and/or crushing of the granule; and (3) reduction of the void volume within the granules by rearrangement of the powder particles. The compaction behaviour examined in this study indicates from SEM observation and mercury porosimetry that compaction

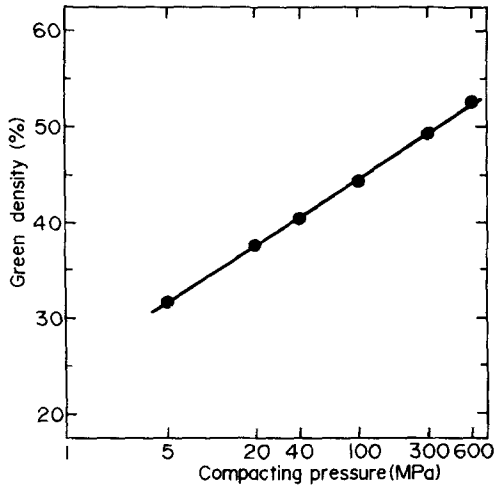

Figure 7 Effect of forming pressure on green density of the powder compact.

stage 2 and/or 3 can be identified in the pressure range applied. The test, however, provided only the net or average change of structure in green compacts, and provided only a little information on minor defects, such as those found by the immersion liquid technique.

It must be clear from the above explanation that the immersion liquid technique has a high ability to characterize internal structure of green compacts. Other than the high resolution of the optical microscope, the high ability of this technique can be attributed to (1) the very large volume examined, (2) a sensitivity to the fluctuation of packing densities, and (3) little damage of the specimen during sample preparation.

The scattering at the particle–liquid interface governs the maximum thickness which can be made transparent. The scattering also affects the contrast of microscopic image. Because the reflection of light, R, is related to the relative refractive index between the particle and the immersion liquid, the adjustment of the refractive index is very important.

Many large processing defects are common to powder compacts examined in this study. These results shows that there is room for improvement in the characteristics of powder compacts examined in this study. The supplier claimed a flexural strength (three-point bending) of 1000 MPa at normal sintering. If the information obtained in this study is fed back into the process to eliminate or control these processing flaws, a still higher strength may be expected for the present material.

Acknowledgements

This research was supported in part by the Science Foundation of the Ministry of Education. The mercury porosimeter at the Niigata Prefecture Industrial Technology Centre was used.

References

1. F. F. LANGE, *J. Amer. Ceram. Soc.* **72** (1989) 3.
2. M. D. WEEKS and J. W. LAUGHER, in "Advances in Ceramics", Vol. 21, "Ceramic Powder Science" edited by G. L. Messing, K. S. Mazdiyasni, J. W. McCauley and R. A. Haber (The American Ceramic Society, Westerville, OH, 1987) pp. 793–800.
3. D. S. KUPPERMAN and H. B. KARPLUS, *Amer. Ceram. Soc. Bull.* **63** (1984) 1505.
4. J. L. ACKERMAN, L. GARRIDO, W. A. ELLINGSON and J. D. WEYAND, in "Nondestructive Testing of High-Performance Ceramics" (The American Ceramic Society, 1987) pp. 88–113.
5. W. D. FRIEDMAN, R. D. HARRIS, P. ENGLER, P. K. HUNT and M. SRINIVASAN, *ibid.*, pp. 128–31.
6. K. UEMATSU, J. Y. KIM, M. MIYASHITA, N. UCHIDA and K. SAITO, *J. Amer. Ceram. Soc.* **73** (1990) 2555.
7. K. UEMATSU, J. Y. KIM, Z. KATO, N. UCHIDA and K. SAITO, *Nippon Seramikkusu Kyokai Gakujuturonbunsi*, **98** (1990) 515.
8. K. UEMATSU, J. Y. KIM, M. MIYASHITA, M. SEKIGUCHI, J. Y. KIM, N. UCHIDA and K. SAITO, *J. Amer. Ceram. Soc.* in press.
9. J. Y. KIM, M. INOUE, Z. KATO, N. UCHIDA, K. SAITO and K. UEMATSU, *J. Mater. Sci.* **26** (1991) 2215.
10. F. F. LANGE and M. METCALF, *J. Amer. Ceram. Soc.* **66** (1983) 398.
11. W. D. KINGERY and B. FRANCOIS, in "Sintering and Related Phenomena", edited by G. C. Kuczynski, N. Hooten and C. Gibson (Gordon and Breach Science, New York, 1976) pp. 471–96.
12. F. F. LANGE, *J. Amer. Ceram. Soc.* **67** (1984) 83.
13. B. J. KELLETT and F. F. LANGE, *ibid.* **72** (1989) 725.
14. G. C. WALL and R. J. C. BROWN, *J. Colloid Interface Sci.* **82** (1981) 141.
15. R. A. YOUSHAW and J. W. HOLLORAN, *Amer. Ceram. Soc. Bull.* **61** (1982) 227.

Received 26 March
and accepted 20 December 1990